European Polymer Journal 220 (2024) 113429

Contents lists available at ScienceDirect

European Polymer Journal

journal homepage: www.elsevier.com/locate/europolj

Copper and ZnO Dual-Catalyzed Photo-Assisted Depolymerization of Poly (Methyl Methacrylate) without Deoxygenation

Martin Cvek [a,b,1], Arman Moini Jazani [a,1], Ferdinando De Luca Bossa [a], Roksana Bernat [a,c], Kriti Kapil [a], Krzysztof Matyjaszewski [a,*]

[a] Department of Chemistry, Carnegie Mellon University, 4400 Fifth Avenue, Pittsburgh, PA 152 13, United States of America
[b] Centre of Polymer Systems, Tomas Bata University in Zlin, Trida T. Bati 5678, 760 01 Zlin, Czech Republic
[c] Institute of Materials Engineering, University of Silesia, 75 Pulku Piechoty 1A, 41-500 Chorzow, Poland

ARTICLE INFO

Keywords:
Depolymerization
ATRP
Polymers
Oxygen
Ligand complexes
Catalyst
Zinc oxide

ABSTRACT

Despite significant advancements in thermal and photothermal depolymerizations, the success of these techniques relies on tedious deoxygenation procedures. Herein, we report the development of the depolymerization technique efficient without prior deoxygenation, which was enabled by copper/ligand complexes and the inclusion (0.25 wt% relative to solvent) of zinc oxide (ZnO) nanocrystals activated by UV light. This approach was tested for poly(methyl methacrylate) (PMMA) prepared by atom transfer radical polymerization (ATRP); the effects of solvent polarity and the activity of ligands were investigated. Unexpectedly, a low-activity Cu-complex with 2,2'-bipyridine ligand, in combination with a low-polarity solvent, 1,2,4-trichlorobenzene, enabled relatively high depolymerization yields in less than 1 h at 150 °C. Higher activity ATRP complexes with tris(2-pyridylmethyl)amine (TPMA) and *N,N,N',N'',N''*-pentamethyldiethylenetriamine (PMDETA) ligands, were less efficient, which was associated with their thermal decomposition and/or the excessive formation of radicals and premature termination of the chain ends. The presented facile approach was designed to be used even in partially aerated reactors, opening new avenues for efficient depolymerization.

1. Introduction

The increasing production of synthetic polymers has created environmental challenges due to the unavailability of efficient (up/re) cycling methods. Mechanical recycling generally yields polymers with deteriorated properties [1] due to undesirable changes in their molecular structure [2]. In comparison, chemical recycling enables theoretically infinite recyclability by generating the starting monomers and reproduction of pristine polymers [3–5].

Polymethacrylates form a remarkable class of polymers with diverse properties that can be tailored by incorporating various functional ester groups into the methacrylic repeat unit [6]. The polymethacrylates exhibit versatile mechanical properties, good weather resistance, excellent optical transparency, etc., which makes them suitable candidates for numerous applications, including engineering plastics, energy storage materials, functional coatings, and biomaterials [6,7]. The most widely used methacrylate monomer, methyl methacrylate (MMA), is produced at 3.9 million tons per year, encompassing a global market valued at USD 7,423 million in 2021, with forecasted growth at a compound annual growth rate (CAGR) of 4.8 % over the period of 2022–2030 [8]. Despite massive production, the waste polymethacrylates are mostly landfilled or incinerated, and only a fraction (10 % in the case of PMMA) of the production is recycled [7]. At the end of their service life, polymethacrylates can be deconstructed at high temperatures (375–500 °C) by pyrolysis, which is energetically costly and commercially demanding [9,10]. Degradation of polymethacrylates is possible by introducing degradable linkages into the initiators [11,12], copolymerization with cyclic monomers via radical ring-opening polymerization (rROP) [13–19], or by β-carbon fragmentation [20–23]. Nevertheless, these methods do not allow the generation of reusable monomers and only disintegrate polymers into smaller fragments.

Depolymerization is an endothermic process in which polymers undergo depropagation to yield monomer units [24–26]. The recovered monomers can be used to synthesize new polymers without deteriorating their properties [9]. The capability of polymers to depolymerize is

* Corresponding author.
E-mail address: km3b@andrew.cmu.edu (K. Matyjaszewski).
[1] These authors contributed equally to this work.

https://doi.org/10.1016/j.eurpolymj.2024.113429
Received 24 July 2024; Received in revised form 30 August 2024; Accepted 31 August 2024
Available online 2 September 2024

dictated by the thermodynamics of polymerization/depolymerization given by the Gibbs free energy (ΔG) [27]. Typically, depolymerization is favored for $\Delta G>0$, while a dynamic equilibrium of both processes is achieved for $\Delta G=0$, which exists at a certain temperature, termed the ceiling temperature (T_C) [28]. Increasing the temperature above T_C can favor depolymerization. However, it is not the only relevant factor affecting the successful depolymerization [24]In practice, other factors include the ability to generate active centers needed for depolymerization, the polymer structure, its initial concentration, the degree of polymerization (DP), the type of solvent and catalyst used, etc. [24,28,29].

Therefore, critical for low-temperature depolymerization is the incorporation of easily cleavable (also under catalytic conditions) moieties at the polymer chain end,[26] notably carbon-heteroatom ($C(sp^3)$–X) bonds (i.e., C-Cl, C-Br, C-S or C-ON bonds) due to their lower energy barrier for generating a radical than from the highly stable $C(sp^3)$–$C(sp^3)$ bond [26,30,31]. Such homolytically cleavable moieties can be readily introduced to the chain ends by reversible-deactivation radical polymerization (RDRP) techniques, most commonly by atom transfer radical polymerization (ATRP) [32], reversible addition-fragmentation chain transfer (RAFT) polymerization [33], and nitroxide-mediated polymerization (NMP) [34].

As reported previously, ruthenium-catalyzed depolymerization of a chlorine-capped poly(methyl methacrylate) (PMMA-Cl) provided relatively low yields, but using the iterative evaporation of monomer the amount of regenerated MMA increased to 15 % within 40 h at 100 °C [26]. Depolymerization of chlorine-capped poly(poly(dimethylsiloxane) methacrylate) (P-PDMS$_{11}$MA)-Cl, poly(n-butyl methacrylate) (PBMA-Cl), and PMMA-Cl using a copper(II) chloride/tris(2-pyridylmethyl) amine ($CuCl_2$/TPMA) complex resulted in a monomer recovery yield in the range of 67–81 % (at 170 °C) [27,35]. This catalytic system also enabled fast bulk depolymerization via short-path distillation and efficient extraction of the recovered monomer (84 % monomer recovery at 230 °C) [36]. Finally, depolymerization of PBMA-Cl and PMMA-Cl mediated with $FeCl_2$ and zero-valent iron, as more environmentally friendly transition metals, provided monomer recovery above 70 % (at 170 °C) [37].

Progress in depolymerizations was also reported for polymers synthesized by the RAFT technique, including polymethacrylates with bulky substituents [31], as well as bottlebrushes [38]. The effects of the end-group, degree of polymerization (DP), and solvents on the depolymerization efficiency of various RAFT poly(meth)acrylates have been reported [29], and remarkable yields, over 90 %, were achieved when working under highly dilute conditions (5 mM). All the mentioned examples suffer from the degradation of chain end functionality, namely lactonization for ATRP and Chugaev elimination for the RAFT technique [36,39,40]. To overcome the limitation given by the loss of chain-end functionality, another approach exploited thermally labile α- and ω-chain ends, or the combination of the two, in a near-quantitative bulk depolymerization of PMMA [41]. A phthalimide-based monomer was employed as a comonomer in a copolymer with MMA, initiating the depolymerization from several points along the backbone, achieving 84 % conversion at 250 °C in 2.5 h [42]. A parallel strategy was recently reported in which low-ceiling temperature monomers were copolymerized with high-ceiling temperature comonomers, such as MMA. This method induced depolymerization at the chain's midpoint due to the weakening of C–C bonds in the backbone [43].

In recent years, significant attention was paid to harnessing light for mediating RDRPs due to its relative abundance, energy efficiency, safety, programmable intensity and wavelength, and ability to spatially and temporally control the polymerization [44,45]. In regards to photodepolymerization, a few attempts were made to increase the efficiency of the depolymerization process by employing photocatalytic systems or light itself to activate the polymer chain-ends. A metastable dimanganese decacarbonyl ($Mn_2(CO)_{10}$) was used as a radical source to depolymerize the PMMA derivatives prepared by ATRP using visible light radiation, but a very low yield (up to 20 %) was obtained [46]. For the RAFT polymers, depolymerization of PMMA by photolysis of its terminal groups, such as trithiocarbonate, dithiocarbamate, and *p*-substituted dithiobenzoate, was facilitated by light at different wavelengths [47]. Importantly, the external light energy mostly served as the accelerating factor, and the contribution of thermal depolymerization was more efficient, making temporal regulation difficult. This challenge has been recently resolved by using iron-based catalysts in ppm amounts, which enabled excellent temporal control of the depolymerization of poly (benzyl methacrylate) (PBzMA) [48]. Additionally, the photoinduced electron/energy transfer (PET)-RAFT depolymerization catalyzed by eosin Y in various solvents has also been investigated [49] and found efficient for temporal control depolymerizations [50].

Despite significant progress in the depolymerization of polymers obtained by RDRP techniques, some relevant factors, such as oxygen sensitivity, have not yet been investigated in depth. Triplet oxygen is a strong quencher of organic radicals and inhibits radical (de)polymerization. In addition, in classical Cu-catalyzed ATRP, oxygen inhibits polymerization by oxidizing the Cu^I/L activator to its inactive form, the Cu^{II}/L complex. This has spurred efforts to develop oxygen-tolerant ATRP systems in recent years [51]. Similarly, in depolymerization, oxygen molecules can oxidize the Cu^I/L activator and quench the propagating radicals, thus inhibiting depolymerization [24]. Although the solubility of oxygen in (meth)acrylates and other organic compounds decreases with temperature, the residual oxygen molecules have a high reactivity towards radical species, quenching their activity [52]. For this reason, depolymerizations are very often performed after thorough deoxygenation, usually achieved by freeze–pump–thaw (FPT) cycles [27] or nitrogen purging [49]. Due to the high oxygen sensitivity, the depolymerization methods are laborious and relatively far from industrial adoption. Recent trials to depolymerize PMMA without deoxygenation using zinc tetraphenylporphyrin (ZnTPP) as external photocatalyst yielded low monomer recovery (below 31 %), which was attributed to the degradation of the RAFT end-group [53].

In a very recent report, the effect of low-boiling point cosolvents on the depolymerization of PBzMA at 170 °C was investigated. This approach benefited from the boiling cosolvents during the reaction that removed dissolved oxygen through the bubbles generated by boiling a solvent, allowing open-air depolymerization with high depolymerization yields (of 76–87 %, depending on the monomer repeat unit concentration) [54]. The oxygen removal was, however, a short-lived event, since after a few minutes, the oxygen started to re-diffuse into the solution. Therefore, such an open-air methodology is feasible for relatively rapid depolymerizations [54].

In this paper, we sought to develop a new depolymerization method that does not require prior deoxygenation and is applicable for longer depolymerization times at relatively low depolymerization temperatures (150 °C), which are factors relevant for the larger scale synthesis. We used a solvent with a high boiling point that previously yielded negligible (>5%) conversion [54]. The dissolved oxygen was efficiently removed by the irradiated zinc oxide (ZnO) nanocrystals, making depolymerization possible in a partly aerated closed reactor, facilitating workflow, and preventing accidental splashes of boiling cosolvents.

Ligands play a major role in controlling ATRP by solubilizing Cu salts, adjusting their redox potentials, and facilitating activation and deactivation via dynamic halogen exchange [55–59]. However, the effects of amine-based ligands on depolymerization have remained underexplored [24]. We postulated that ligands contribute to depolymerization at high temperatures by controlling the extent of radical generation and acting as electron donors to both the photo-excited and ground states of the Cu/ligand complexes. Therefore, the stability of Cu/ligand complexes at higher temperatures dictates the availability of catalysts for polymer end-chain activation.

Recently, we reported that the UV-irradiated ZnO nanocrystals dispersed in dimethyl sulfoxide (DMSO) (boiling point, b.p., of 189 °C) can trigger a cascade of photocatalytic reactions, enabling rapid removal

of dissolved oxygen while generating dimethyl sulfone ($DMSO_2$) [60]. Inspired by this finding, we tested this protocol for the photo-assisted depolymerization of PMMA-Cl prepared by ATRP (Scheme 1) and extended its applicability to other high-boiling point solvents, such as 1,2,4-trichlorobenzene (TCB) (b.p. of 213 °C).

2. Results and discussion

2.1. Depolymerization of PMMA in the presence of different Cu complexes in DMSO and TCB

The selection of an appropriate halogen chain-end of PMMA is important for efficient depolymerization. As recently reported [35,46], the depolymerization of PMMA with a bromine chain-end (PMMA-Br) led to termination reactions such as lactonization since Br is a good leaving group. Although depolymerization of Br-terminated polymers, such as PBzMA, has recently been optimized toward high efficiencies [61], in the case of PMMA, the chlorine chain end (PMMA-Cl) was reported to provide higher yields because of the stronger C–Cl bond. For this reason, PMMA-Cl ($M_{n,\,GPC}$=5100, $Đ = 1.24$, DP=54) synthesized via the initiators for continuous activator regeneration (ICAR) ATRP was selected as a model polymer. The chain-end functionality of PMMA-Cl was estimated to be 85 %, determined by chain-extension experiments [37].

The experimental setup consisted of an aerated reaction vessel with 20 % of the headspace partially immersed in an oil bath and exposed to UV irradiation (380 nm, 28.5 mW/cm^2) (technical details; ESI, Section 1.4). The effect of three common ATRP ligands, such as TPMA [62], N,N,N′,N″,N″-pentamethyldiethylenetriamine (PMDETA) [62,63], and 2,2′-bipyridine (BPY) [64], on depolymerization was investigated under equimolar conditions of [PMMA-Cl]/[$CuCl_2$]/[ligand] = 1/1/1 at 150 °C. At this temperature, the equilibrium monomer concentration of methyl methacrylate, $[MMA]_{eq}$, was calculated to be 0.158 M following the scaling function [36,65], and using the thermodynamic parameters; ΔH_p of –56 kJ/mol and ΔS_p° of –117 J/mol·K [25]. The depolymerization progress was monitored by gel permeation chromatography (GPC) and proton nuclear magnetic spectroscopy (^{1}H NMR) (ESI, Section 1.7., **Figure S1, S2**). The conversion determined by GPC was generally higher than that calculated by ^{1}H NMR, but was considered less accurate since we could not use polystyrene (PS) and poly(ethylene glycol) (PEG) as the conventional internal standards due to their degradation under UV light at high temperatures (ESI, Section 2.2.). The

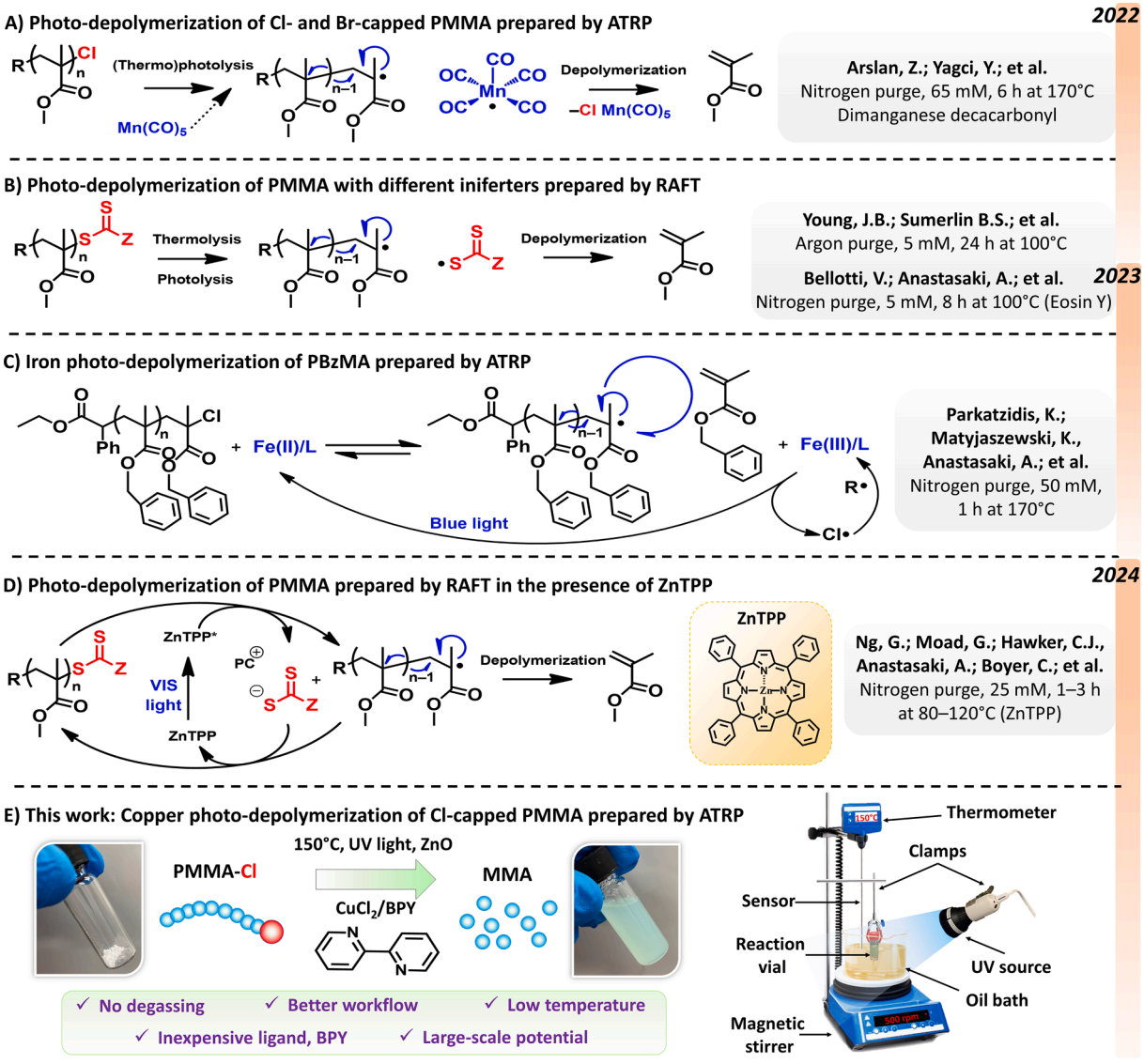

Scheme 1. The overview of reported photothermal depolymerizations of PMMA and PBzMA prepared by RDRPs and performed under an inert atmosphere [46–49,53], including the reported herein technique that does not require prior deoxygenation, with the highlighted improvements.

discrepancy between the ^{1}H NMR and GPC data could be attributed to the formation of oligomers that were not detectable by the GPC; hence, they decreased the PMMA peak area, or less likely, a loss of MMA during depolymerization at relatively high temperatures before ^{1}H NMR analysis. For these reasons, the GPC data served as a less precise estimate for the depolymerization, while conversion in terms of the recoverable MMA was calculated from ^{1}H NMR spectra (**Figure S2**). A broader comparison is included in the ESI (Section 2.2. and 2.3.).

Screening of the kinetics for ZnO-mediated UV-assisted depolymerization with different ligands was performed (**Figure S3**). In all cases, the depolymerization yield increased rapidly within 30 min and then plateaued without further progression after 60 min, which was the representative time for our depolymerization experiments (Fig. 1**A**). The depolymerization yield values depended on the Cu complexes' activity with various ligands. For the TPMA, a NMR conv. of 19 % was achieved, while the less active ligand, PMDETA, yielded a NMR conv. of 24 % within 60 min. The use of BPY increased the NMR conv. up to 28 % under identical conditions. The representative GPC traces, taken after 60 min, are displayed in Fig. S3A.

To expand the scope of solvents, we used TCB as a solvent for the ZnO-mediated UV-assisted depolymerization. In this case, the depolymerization yield increased significantly compared to those for DMSO regardless of the ligand type (Fig. 1**B and S3B**), which was associated with the lower polarity of this solvent, a lower concentration of radicals and suppressed lactonization in less polar media. The effect of the ligand on depolymerization followed a similar trend as for the DMSO-based systems; however, in this case, the highest NMR conv. reached 46 % for BPY in 60 min. The minimal change in the shape and positions of the GPC traces suggests that uncontrolled unzipping was a predominant mechanism. Overall, the highly active ligands generated excess radicals that underwent more termination, thus ceasing the depolymerization [29].

2.2. Comparison of depolymerization under thermal and photothermal conditions

Then, we explored the effect of UV light on depolymerization efficiency by performing exclusively thermal depolymerizations. When using TPMA and PMDETA as ligands (Fig. 1**C**), the depolymerizations proceeded even in the absence of UV light with relatively moderate NMR conv. values of 36 % and 42 %, respectively. Interestingly, the thermal depolymerization with TPMA showed a slightly higher efficiency when compared to its photothermally activated conditions (Fig. 1**C vs. 1B**). Plausibly, a highly active TPMA complex in combination with UV-irradiated ZnO promoted the excessive production of radicals and premature termination of the chain ends (Vide infra, UV–VIS). This phenomenon was reduced by removing the light activation, thus prolonging the fidelity of the chain ends.

Depolymerization with BPY occurred only when both UV light and heat were applied simultaneously (photothermal activation) (Fig. 1**C vs. 1B**). These results demonstrate that depolymerization in the presence of $CuCl_2$/BPY proceeded only via electron transfer from ZnO to the $CuCl_2$/BPY complex because pyridine nitrogens are poor electron donors [66]. Conversely, free TPMA and PMDETA can serve, upon heating, as electron donors, reducing the excited Cu(II) deactivators to Cu(I) activators via the classical photoATRP mechanism and reductive quenching of excited Cu(II)/ligand. In addition, TPMA and PMDETA can reduce ground-state Cu(II)/L species (in dark) at elevated temperatures via the ARGET mechanism.

A series of control experiments was performed with the most relevant

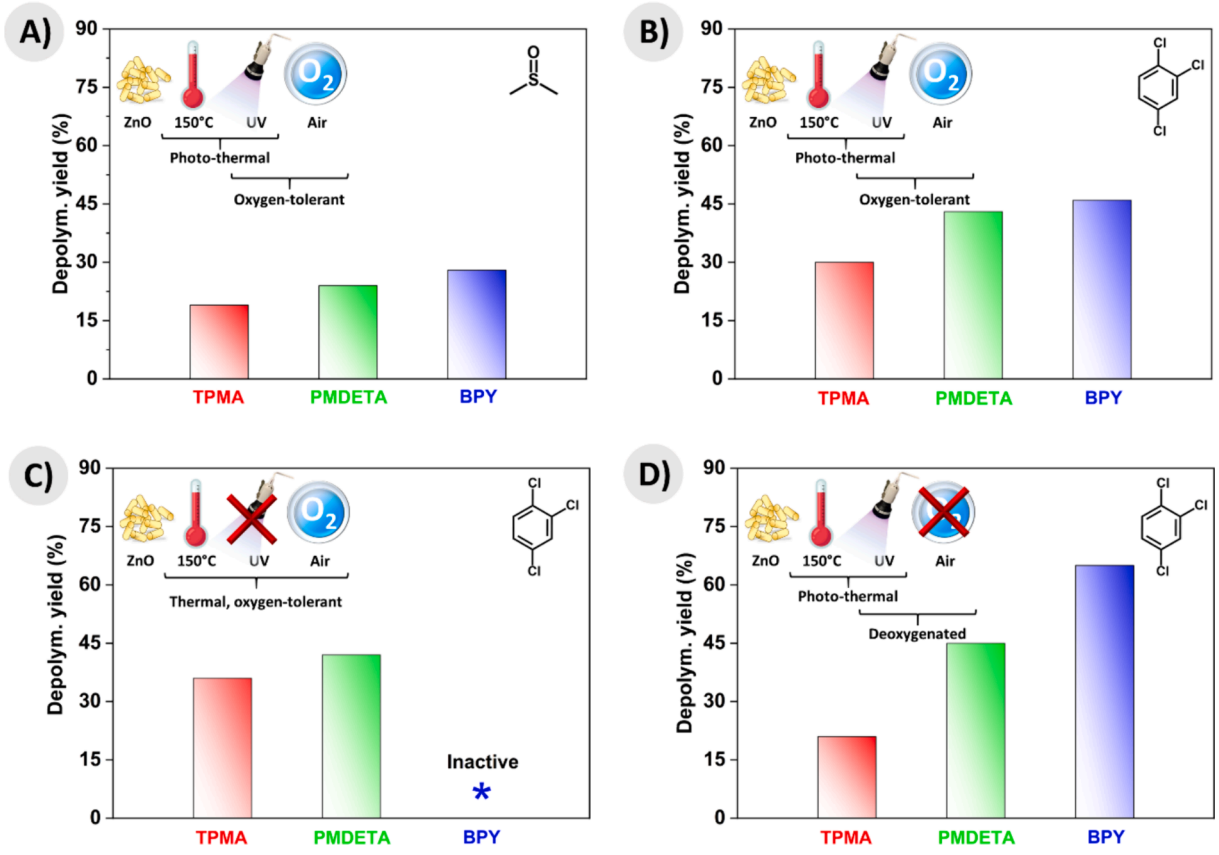

Fig. 1. Comparison of (photo)thermally activated (heterogeneous) depolymerizations of PMMA-Cl (DP of 56) with different ligands in DMSO (A) and TCB (B, C, and D) without prior deoxygenation (A, B, and C) and under deoxygenated (D) conditions in terms of the conversion (determined by ^{1}H NMR). Reaction conditions: $[PMMA\text{-}Cl]_0/[CuCl_2]_0/[ligand]_0$ = equimolar, reaction time of 60 min at 150 °C, UV irradiation (380 nm, 28.5 mW/cm^2), ZnO loading of 0.25 wt% relative to solvent, reaction volume of 3.84 mL (20 vol% aerated headspace).

oxygen-tolerant recipe (Fig. 1**B**, BPY as a ligand) to gain a deeper insight into the role of the individual ATRP components. In the separate experiments, depolymerizations in the absence of ZnO, ligand (BPY), and $CuCl_2$ yielded a negligible conversion (<3%, calculated by ^{1}H NMR) in all the cases (**Table S1**, Entries 1–4). This suggests that the ZnO catalyst, as well as the $CuCl_2$/BPY complex, are necessary for successful depolymerization [36]. Also, it should be noted that the Cu complexes typically exist in their stable $Cu^{I}(BPY)_2^{+}$ form [67], which implies that only half could be catalytically active when using the equimolar $CuCl_2$/BPY=1/1 concentration. The other half formed much less active anionic $CuCl_2^-$ species [55,68]. For this reason, we examined the effect of the Cu/BPY ratio on the efficiency of photothermal depolymerizations with ZnO (**Table S1**, Entries 5–7). In the case of $CuCl_2$/BPY=1/2, the NMR conv. decreased, most likely due to the increased solubility of copper salt and the higher electron-donating effect, which promoted the termination reactions. Upon decreasing the $CuCl_2$/BPY concentration to 1/0.5, the depolymerization yield changed rather minimally; however, more detailed optimizations are necessary to identify the optimal Cu/L loading.

2.3. The effect of oxygen on depolymerization

The tolerance to oxygen in ZnO/$CuCl_2$/L catalytic systems is achieved via two mechanisms: (i) the classical photo-ATRP mechanism via the reaction of oxygen with Cu(I) or the radicals in PMMA chain ends; (ii) ZnO-induced electron transfer to O_2 and the formation of a superoxide radical anion ($O_2^{\cdot-}$), which can further react with the solvent (i.e., DMSO), or Cu(I) species [69–71]. To investigate the effect of oxygen, depolymerizations in TCB were performed after conventional deoxygenation via nitrogen purging [48]. As seen in Fig. 1**D**, the depolymerization yield increased under inert conditions, when either PMDETA or BPY were used, reaching NMR conv. values of 45 % and 65 %, respectively. On the contrary, depolymerization under deoxygenated conditions using TPMA as a ligand yielded lower efficiency compared to the standard conditions without deoxygenation (Fig. 1**D vs. 1B**). This suggests that the presence of oxygen reduced the radical concentration, possibly via the formation of transient peroxy species, and suppressed termination induced by the high activity of TPMA.

We can also attribute such phenomena to different timescales of depolymerization/deoxygenation processes. As shown in **Figure S3**, depolymerizations employing $CuCl_2$/PMDETA and $CuCl_2$/TPMA complexes proceed almost immediately upon immersing the reaction vial into the heated bath; however, a longer time was needed for complete oxygen removal via the UV-irradiation with ZnO (ESI, Section 2.4., **Figure S5**). Therefore, the onset of the depolymerization process most likely happens before the complete elimination of oxygen. The residual oxygen might cause undesirable termination of the PMMA chain ends, and therefore, nitrogen purging enhanced the efficiency of the ZnO co-catalyzed (photo)depolymerizations.

2.4. Stability of Cu/L complexes at high temperatures

To understand the mechanism of Cu-based depolymerization in the presence of O_2, the stability of the $CuCl_2$/ligand complexes was periodically monitored via Vis-NIR spectroscopy upon exposure to a temperature of 150 °C (Fig. 2). The spectra for $CuCl_2$/BPY and $CuCl_2$/TPMA complexes exhibited a 30 % and 20 % reduction in the λ_{max} absorbance within 60 min, respectively, implying their decomplexation and formation of bare ligands and $CuCl_2$ species. At such a state, the bare ligands can act as either electron donors to the remaining $CuCl_2$/ligand complexes or activate PMMA-Cl via supplemental activation [35,72,73]. After returning the solutions to ambient temperature, the optical properties of the $CuCl_2$/BPY and $CuCl_2$/TPMA complexes significantly recovered. The regeneration of the complex of tetradentate TPMA was,

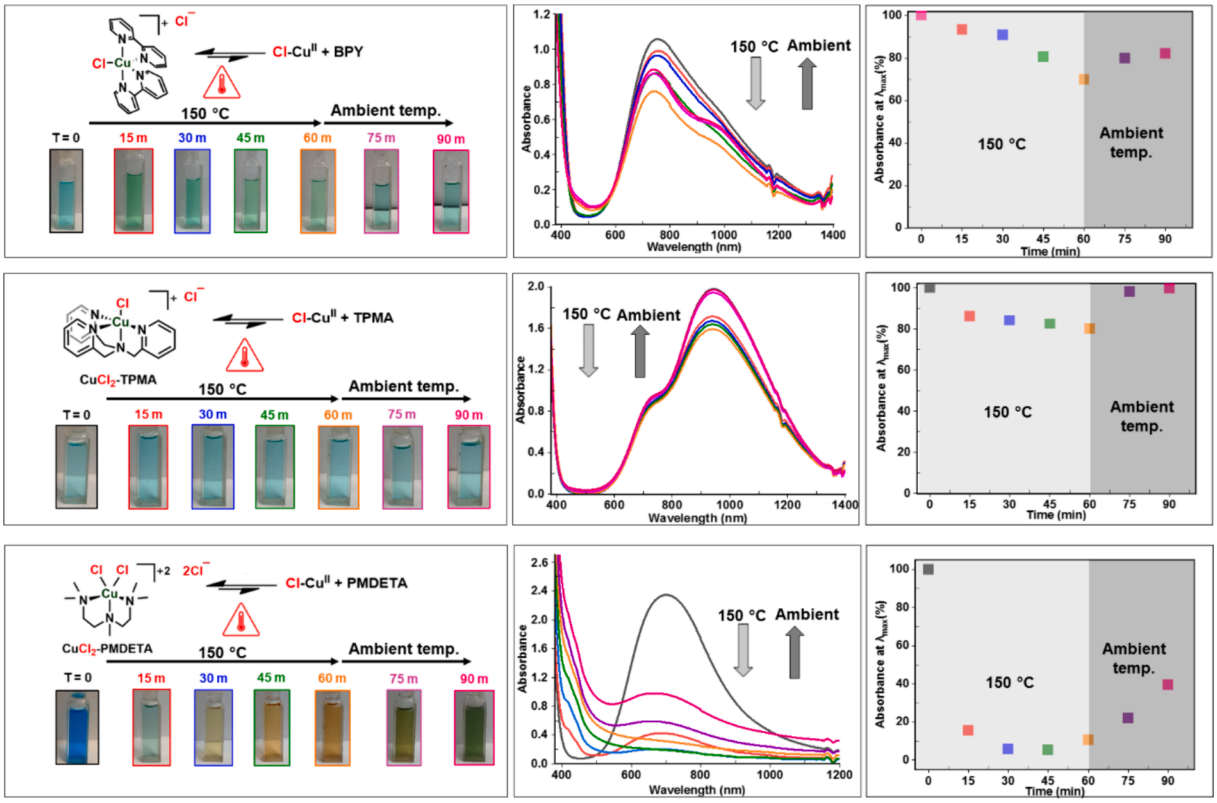

Fig. 2. The evolution of the color (left), the corresponding Vis-NIR spectra at different times (middle), and the peak absorption (λ_{max}) plotted as a function of time (right) for BPY (A), TPMA (B), and PMDETA (C) of $CuCl_2$/ligand solutions (12.4 mM) upon heating to 150 °C (60 min) and subsequent exposure to ambient temperature (30 min). $[CuCl_2]_0/[ligand]_0 = 1/1$ in DMSO without prior deoxygenation.

however, faster and more pronounced (recovery to 99.5 % of λ_{max}) compared to that of bidentate BPY (recovery to 82 % of λ_{max}).

The $CuCl_2$/PMDETA complexes showed the most significant and fastest drop in absorption values (95 % reduction of λ_{max} within 15 min), accompanied by intense color changes (Fig. 2). Such a phenomenon likely indicates the formation of both naked $CuCl_2$ and PMDETA, as well as a reduction to CuCl by PMDETA. Unlike TPMA and BPY, the recovery of PMDETA complexes was slow and incomplete upon keeping the solutions at ambient temperature. Furthermore, the blue shift in λ_{max} from 705 to 657 nm in the $CuCl_2$/PMDETA spectrum, along with the irreversible color change from blue to dark green, suggested the decomposition of PMDETA and the formation of new species.

Next, the stability of all three ligands and the possibility of side reactions at 150 °C were investigated using ^{1}H NMR spectroscopy in DMSO-d_6. The ^{1}H NMR spectrum for BPY remained nearly invariant after 60 min of thermal incubation (**Figure S6**), whereas the ^{1}H NMR spectrum for PMDETA showed new peaks (6.5–7.5 ppm and 1.2–1.3 ppm), suggesting the generation of side products (**Figure S7**). In the case of TPMA, the formation of 2-pyridinecarboxaldehyde (10.0 ppm) and other minor products (1.2–1.4 ppm and 2.7–2.9 ppm) was detected, suggesting its thermal instability in the presence of air (**Figure S8**). It is also noteworthy that such chemical transformation may be promoted or suppressed in the presence of Cu or light, which has a significant impact on the depolymerization process (Fig. 1).

2.5. Effect of oxygen and light on reduction of $CuCl_2$/L complex

Then, the effects of UV irradiation and deoxygenation on the Vis-NIR spectra of $CuCl_2$ complexes were investigated. As shown in Fig. 3, deoxygenation (nitrogen purge) resulted in the highest reduction in the absorption peaks of all three complexes. This can be attributed to an increase in the formation of Cu(I) activators, which are typically oxidized to Cu(II) in the presence of O_2. In addition, UV light also promoted the reduction of $CuCl_2$/BPY and $CuCl_2$/TPMA complexes, suggesting that detached ligands may act as electron donors in the photoreduction of excited Cu(II)/L species [74,75]. In the case of $CuCl_2$/BPY, it was assumed that decomplexed BPY reduced the remaining complexes (Fig. 3), but its limited electron-donating ability was insufficient to activate PMMA-Cl via supplemental activation (Fig. 1**C**). Interestingly, $CuCl_2$/PMDETA complexes displayed higher absorbance values under photothermal conditions compared to exclusively thermal conditions. Overall, these results suggest that PMDETA is rather a poor ligand for high-temperature depolymerizations due to its insufficient thermal stability, whereas BPY and TPMA are relatively stable at higher temperatures necessary to carry out depolymerization.

2.6. Bulk depolymerization

The versatility and robustness of the depolymerization system were examined by carrying out solvent-free (bulk) depolymerization of PMMA-Cl using the selected catalytic system, $CuCl_2$/BPY/ZnO, that provided the highest yield in depolymerization (Fig. 1**D**, BPY). The bulk depolymerization was carried out using 500 mg of PMMA, i.e., 10x higher than in the experiments performed in the previous sections. PMMA-Cl prepared by ICAR ATRP was reversed to monomers upon 30 min of UV light irradiation at 200℃, while the monomer was separated from the depolymerization reactor by vacuum distillation to prevent its (re)polymerization (Fig. 4). The depolymerization yield, calculated based on the loss of PMMA weight in the distillation flask, reached 62 %. This amount corresponded to 90 % MMA recovery, i.e., the weight fraction of the obtained monomer based on the weight loss of the polymer, [36] as confirmed by ^{1}H NMR (Fig. 4**E**). The MMA isolated by this method was used to copolymerize with n-butyl methacrylate using PET-RAFT polymerization, demonstrating the possibility to convert MMA into (co)polymers by another RDRP technique [76,77]. The control experiment without ZnO yielded only an 11 % yield of MMA (91 % monomer recovery), confirming the key role of ZnO in reducing $CuCl_2$ and driving depolymerization. In addition, another control experiment performed without $CuCl_2$/BPY (only with ZnO) did not show significant changes in the polymer's mass, underscoring the importance of the dual catalysis of $CuCl_2$/BPY for depolymerization.

2.7. Mechanism of depolymerization with ZnO

The activation mechanism of the polymeric chain-ends of PMMA-Cl is summarized in Scheme 2. Accordingly, three possible pathways for the reduction of Cu(II)/L to Cu(I)/L species are possible: (1) exclusively thermal (in the dark) reduction of the ground state Cu(II)/L; (2) photo-

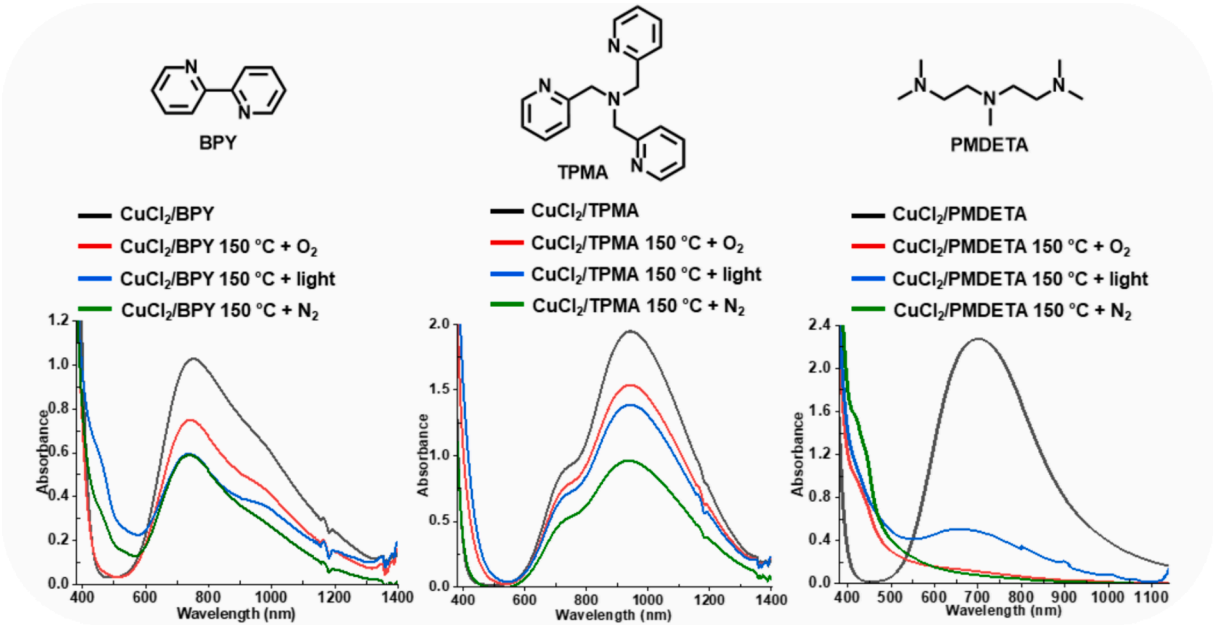

Fig. 3. Vis-NIR spectra of $CuCl_2$/ligand solutions (12.4 mM) before any treatment, upon heating to 150 °C in an oxygen/nitrogen atmosphere, and under UV irradiation (380 nm, 28.5 mW/cm^2). $[CuCl_2]_0/[ligand]_0 = 1/1$ in DMSO.

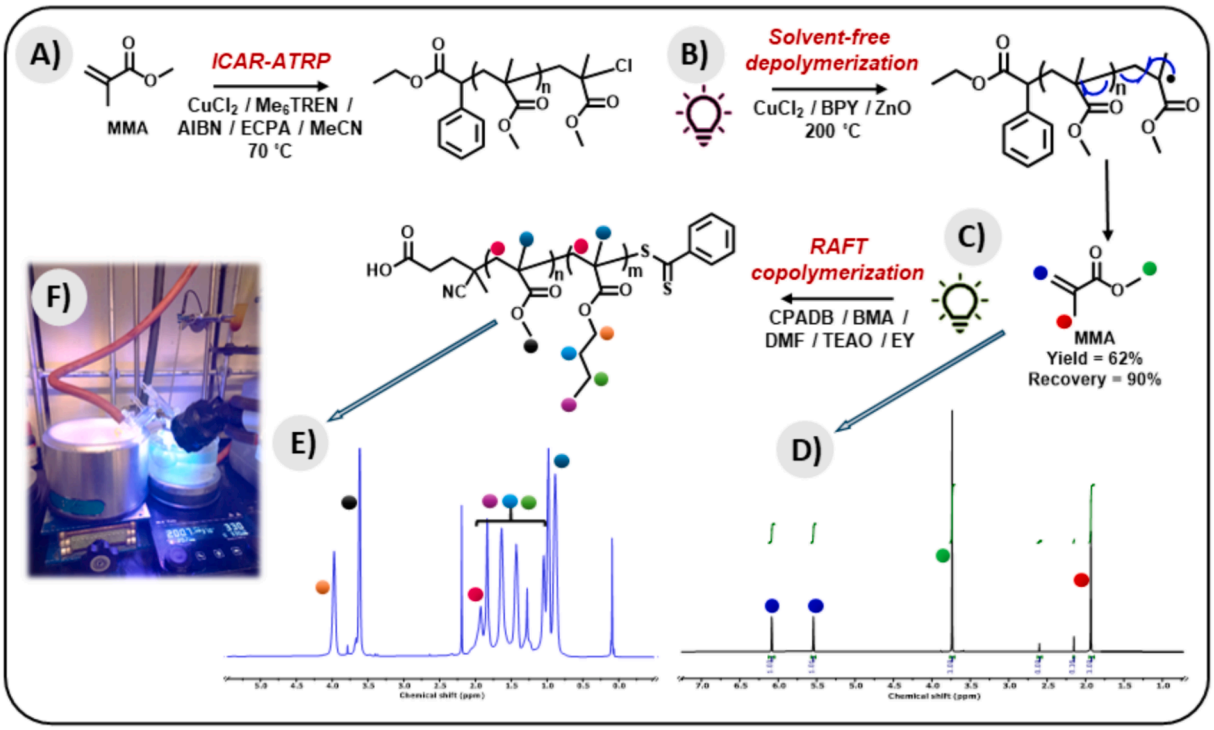

Fig. 4. General scheme for the synthesis of PMMA-Cl by ICAR ATRP (A), depolymerization to MMA using $CuCl_2$/BPY/ZnO (B), and copolymerization of the recovered MMA with BMA by PET-RAFT polymerization (C). ^{1}H NMR spectra for recovered MMA after depolymerization (D) and purified poly(MMA-co-BMA) copolymers in $CDCl_3$ (E). The experimental set-up for bulk depolymerization of PMMA-Cl (F). AIBN: Azobisisobutyronitrile; ECPA: Ethyl α-chlorophenylacetate; MeCN: Acetonitrile; BMA: n-Butyl methacrylate; CPADB: 4-Cyano-4-(phenylcarbonothioylthio)pentanoic acid; TEAO: Triethanolamine; EY: Eosin Y; DMF: Dimethylformamide.

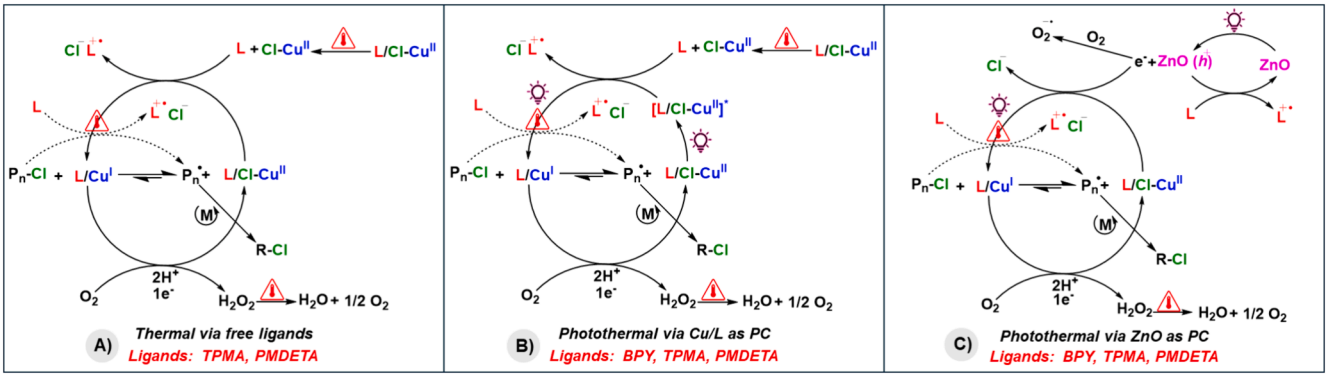

Scheme 2. Mechanism of depolymerization of PMMA-Cl with $CuCl_2$/L complex: in the absence of UV light (A), in the presence of UV light (B), and in the presence of ZnO and UV light (C).

reduction of the excited state [Cu(II)/L]* by de-complexed (free) ligands; and (3) photo-reduction of the ground and excited state Cu(II)/L complex with electrons generated from excited [ZnO]*. In the absence of UV light, free ligands released from Cu(II)/L at higher temperatures reduce the remaining Cu(II)/L complex, generating Cu(I)/L complex as well as amine radical cations ($L^{\bullet+}$, Scheme 2**A**). Such free ligands reduce excited [Cu(II)/L]* more readily, because it has a much more positive oxidation potential (e.g., +2.07 V vs. −0.23 V for [Br-Cu^{II}/TPMA)$^+$]* and [Br-Cu^{II}/TPMA)$^+$]) (Scheme 2**B**) [78].

The amine radical cations decompose to iminium ions that remain innocent in polymerization/depolymerization [79]. As described earlier (Fig. 1**C**), BPY could not induce depolymerization without ZnO since the aromatic amines in BPY are not good electron donors to reduce Cu(II)/L, unlike PMDETA and TPMA, which reduced both the ground and excited states of Cu(II)/L. Therefore, Cu(II)/BPY is mainly reduced by electrons (e^-) generated from the photoexcitation of ZnO, which also forms electron holes (h^+) upon excitation (Scheme 2**C**) [35,36,80].

Consequently, most chains of PMMA-Cl are activated by the Cu(I)/L complex. However, some direct activation of chains by amine ligands via the formation of a halogen-bonding complex is also possible (dashed arrows) [35], which is facilitated at high temperatures and in the presence of light [81]. Ligand may also induce the elimination reaction of the PMMA-Cl end-group while forming an unsaturated vinyl end-chain (macromonomers), which may undergo depolymerization even more readily [40]. The model reactions of alkyl halide and ligands proved the formation of vinyl peaks at 5.7 and 6.1 ppm in ^{1}H NMR spectra (**Figure S9**). The extent of elimination increases in the order of PMDETA>TPMA>BPY, which correlates with the basicity and number of alkyl amines in the ligands. Considering the high temperatures and relatively low monomer concentration used in these experiments, the

thermodynamic conditions favor depolymerization over polymerization, and the unzipping of the polymer chains results in the formation of monomers.

Finally, despite the poor solubility of oxygen in solvents at high temperatures, the traces of oxygen in the depolymerization solution acted as either an inhibitor (i.e., BPY) or a promotor of the depolymerization. The oxygen tolerance is rendered to this system mostly by Cu(I)/L, which reacts with oxygen (O_2), (re)generating Cu(II)/L and H_2O_2. Moreover, free electrons (e^-) generated from the photoexcitation of ZnO could form superoxide anions ($O_2^{\bullet-}$). Oxygen O_2 is also scavenged by reacting with PMMA end group radicals, forming peroxide end groups [69]. Due to the instability of peroxy species at high temperatures, they decompose to H_2O and O_2 or undergo a Cu-catalyzed Fenton-like reaction and form hydroxyl radicals ($OH^{\bullet}$). The formed reactive oxygen species (ROS) (superoxide anion and hydroxyl radicals) may further react with DMSO or a ligand. Importantly, no side products from the reaction of MMA with oxygen at a higher temperature were detected in ^{1}H NMR. This is contrary to some other vinyl monomers (e.g., styrene) that form oxidized products (e.g., benzaldehyde or benzoic acid) at high temperatures during aerobic depolymerization [82,83].

2.8. A broader perspective

Previously, high depolymerization yields were reported for poly(meth)acrylates prepared by RDRPs under specific conditions. For example, depropagation was favored by using diluted solutions (5 mM) [31] or relatively high temperatures (190–250 °C) [37,41]. Such a dilution, however, is challenging because of the limited amount of monomer that can be recovered (approx. 5 g of polymer at 5 mM repeating unit requires 10 L of solvent) [40]. We, therefore, aimed to depolymerize polymethacrylate solutions at concentrations close to the equilibrium monomer concentration, which translates into 30-fold higher values (at 158 mM repeating units, i.e., 2.93 mmol PMMA of DP 54) at 150 °C, potentially enabling to depolymerize up to 164 g of PMMA per 10 L of TCB as solvent. The depolymerization yield was correlated with the concentration of repeating monomer units and other relevant parameters (cf. Fig. 5). To address the temperature effects, by comparing our data (Fig. 1**B**, BPY as a ligand) with the depolymerization yield of PMMA-Cl catalyzed by Fe^0 at 150 °C [37], a similar performance was observed. This indicates the comparable efficiency of the presented method, which also benefits from a significantly improved workflow by avoiding deoxygenation.

3. Conclusions

In summary, the depolymerization technique utilizing a high-boiling point solvent and UV-activated ZnO nanocrystals as oxygen scavengers was developed. The depolymerizations were performed without prior deoxygenation in aerated reaction vessels (20 vol% headspace) at relatively concentrated (0.158 M of repeating monomer units at 150 °C) solutions of PMMA-Cl prepared by ATRP. The feasibility was investigated in DMSO and TCB solvents, while TPMA, PMDETA, and BPY were tested as ligands forming ATRP catalysts with different activities. TPMA and PMDETA ligands generated higher concentrations of radicals, promoting a faster loss of chain-end fidelity and thereby inhibiting depolymerization. The copper complexes with PMDETA were thermally unstable, rendering them inefficient for depolymerization. The highest yields were achieved using BPY as a stable and less active ligand, especially in TCB. Unlike TPMA and PMDETA, the BPY allowed efficient photothermal depolymerization. Furthermore, our system was adopted for bulk depolymerization, demonstrating its versatility and large-scale potential. The recovered MMA was copolymerized with BMA using the PET-RAFT technique. Overall, the presented strategy allows for fast depolymerizations with a facile workflow that provides reasonable yields without laborious deoxygenations or the need for expensive or specialized equipment, paving avenues for potential adoption on a larger scale.

CRediT authorship contribution statement

Martin Cvek: Writing – original draft, Formal analysis, Data curation, Conceptualization. **Arman Moini Jazani:** Writing – review & editing, Formal analysis, Data curation, Conceptualization. **Ferdinando De Luca Bossa:** Data curation, Conceptualization. **Roksana Bernat:**

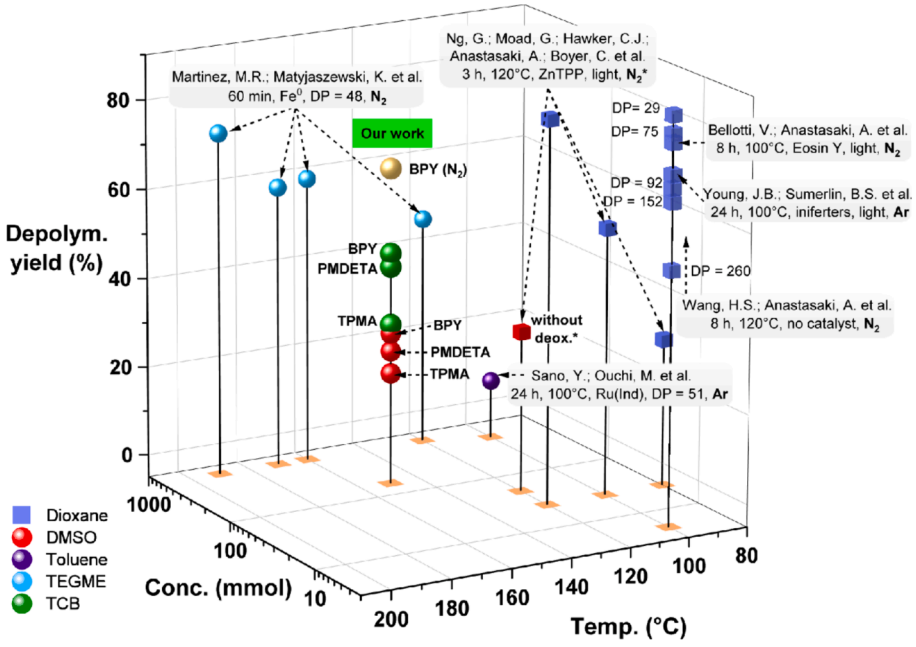

Fig. 5. The overview of the experimental conditions reported for depolymerizations of PMMA prepared by RDRPs (ATRP and RAFT distinguished by spheres and cubes, respectively) executed (mostly) upon deoxygenation. This work: reaction time of 60 min at 150 °C, irradiation (380 nm, 28.5 mW/cm^2), ZnO loading of 0.25 wt% relative to solvent, DP=54, no degassing, aerated headspace (20 % v/v); the optimized depolymerization performed with BPY after prior deoxygenation (BPY, N_2); data based on ^{1}H NMR.

Formal analysis. **Kriti Kapil:** Data curation. **Krzysztof Matyjaszewski:** Writing – original draft, Conceptualization.

Declaration of competing interest

The authors declare the following financial interests/personal relationships which may be considered as potential competing interests: [K Matyjaszewski reports a relationship with National Science Foundation that includes: funding grants. If there are other authors, they declare that they have no known competing financial interests or personal relationships that could have appeared to influence the work reported in this paper.].

Data availability

Data will be made available on request.

Acknowledgements

The financial support from NSF (DMR 2202747 and DMR 2324168) is acknowledged. M.C. is grateful to the J. W. Fulbright Commission in the Czech Republic for the financial support through a postdoctoral fellowship (grant number: 2022-21-1). M.C. further acknowledges the projects DKRVO (RP/CPS/2022/007) and (RP/CPS/2024-28/007) supported by the Ministry of Education, Youth and Sports of the Czech Republic. A.M.J greatly acknowledges the Fonds de recherche du Québec (FRQNT) for financial support (File#301734). R.B. acknowledges financial support from the National Science Centre within the MINIATURA project (DEC-2023/07/X/ST5/01484) and from the Foundation for Polish Science (FNP). The authors acknowledge Dr. Grzegorz Szczepaniak (University of Warsaw) and Dr. Gorkem Yilmaz (Carnegie Mellon University) for fruitful discussions.

Appendix A. Supplementary material

Supplementary data to this article can be found online at https://doi.org/10.1016/j.eurpolymj.2024.113429.

References

[1] K. Hamad, M. Kaseem, F. Deri, Recycling of waste from polymer materials: An overview of the recent works, Polym. Degrad. Stab. 98 (2013) 2801–2812.
[2] M. Cvek, M. Kracalik, M. Sedlacik, M. Mrlik, V. Sedlarik, Reprocessing of injection-molded magnetorheological elastomers based on TPE matrix, Compos. Part B 172 (2019) 253–261.
[3] L. Wimberger, G. Ng, C. Boyer, Light-driven polymer recycling to monomers and small molecules, Nat. Commun. 15 (2024) 2510.
[4] K. Parkatzidis, H.S. Wang, A. Anastasaki, Photocatalytic upcycling and depolymerization of vinyl polymers, Angew. Chem., Int. Ed. 63 (2024) e202402436.
[5] L.H. Kugelmass, C. Tagnon, E.E. Stache, Photothermal mediated chemical recycling to monomers via carbon quantum dots, J. Am. Chem. Soc. 145 (2023) 16090–16097.
[6] P.F. Holmes, M. Bohrer, J. Kohn, Exploration of polymethacrylate structure-property correlations: Advances towards combinatorial and high-throughput methods for biomaterials discovery, Prog. Polym. Sci. 33 (2008) 787–796.
[7] M. Sponchioni, S. Altinok, Poly(methyl methacrylate): Market trends and recycling, in: D. Moscatelli, M. Pelucchi (Eds.), TOWARDS CIRCULAR ECONOMY: Closing the Loop with Chemical Recycling of Solid Plastic Waste 2022, 269-287.
[8] Methyl Methacrylate Market Size - Global Industry Share, Analysis, Trends and Forecast 2022 - 2030, https://www.acumenresearchandconsulting.com/methyl-methacrylate-market, (accessed December 2023).
[9] G.W. Coates, Y. Getzler, Chemical recycling to monomer for an ideal, circular polymer economy, Nat. Rev. Mater. 5 (2020) 501–516.
[10] I.A. Ignatyev, W. Thielemans, B. Vander Beke, Recycling of polymers: a review, ChemSusChem 7 (2014) 1579–1593.
[11] X.L. Hu, A.M. Jazani, J.K. Oh, Recent advances in development of imine-based acid-degradable polymeric nanoassemblies for intracellular drug delivery, Polymer 230 (2021) 124024.
[12] A.M. Jazani, J.K. Oh, Development and disassembly of single and multiple acid-cleavable block copolymer nanoassemblies for drug delivery, Polym. Chem. 11 (2020) 2934–2954.
[13] F. Dawson, T. Kazmi, P.J. Roth, M. Kopec, Strands vs. crosslinks: Topology-dependent degradation and regelation of polyacrylate networks synthesised by RAFT polymerisation, Polym. Chem. 14 (2023) 5166–5177.
[14] M.R. Hill, T. Kubo, S.L. Goodrich, C.A. Figg, B.S. Sumerlin, Alternating radical ring-opening polymerization of cyclic ketene acetals: Access to tunable and functional polyester copolymers, Macromolecules 51 (2018) 5079–5084.
[15] A.M. Jazani, R. Bernat, K. Matyjaszewski, Visible light-induced photo-radical ring-opening copolymerization of thionolactone and acrylates, Polymer 302 (2024) 127032.
[16] C. Lefay, Y. Guillaneuf, Recyclable/degradable materials via the insertion of labile/cleavable bonds using a comonomer approach, Prog. Polym. Sci. 147 (2023) 101764.
[17] T. Pesenti, J. Nicolas, 100th Anniversary of macromolecular science viewpoint: Degradable polymers from radical ring-opening polymerization: Latest advances, new directions, and ongoing challenges, ACS Macro Lett. 9 (2020) 1812–1835.
[18] A. Tardy, J. Nicolas, D. Gigmes, C. Lefay, Y. Guillaneuf, Radical ring-opening polymerization: Scope, limitations, and application to (bio)degradable materials, Chem. Rev. 117 (2017) 1319–1406.
[19] S. Zhang, C. Cao, S.Q. Jiang, H.C. Huang, A general strategy for radical ring-opening polymerization of macrocyclic allylic sulfides, Macromolecules 55 (2022) 9411–9419.
[20] T. Kimura, K. Kuroda, H. Kubota, M. Ouchi, Metal-Catalyzed switching degradation of vinyl polymers via introduction of an "in-chain" carbon-halogen bond as the trigger, ACS Macro Lett. 10 (2021) 1535–1539.
[21] A. Adili, A.B. Korpusik, D. Seidel, B.S. Sumerlin, Photocatalytic direct decarboxylation of carboxylic acids to derivatize or degrade polymers, Angew. Chem., Int. Ed. 61 (2022) e202209085.
[22] H. Makino, T. Nishikawa, M. Ouchi, Incorporation of a boryl pendant as the trigger in a methacrylate polymer for backbone degradation, Chem. Commun. 58 (2022) 11957–11960.
[23] S. Yamamoto, T. Kubo, K. Satoh, Interlocking degradation of vinyl polymers via main-chain C-C bonds scission by introducing pendant-responsive comonomers, J. Polym. Sci. 60 (2022) 3435–3446.
[24] G.R. Jones, H.S. Wang, K. Parkatzidis, R. Whitfield, N.P. Truong, A. Anastasaki, Reversed controlled polymerization (RCP): Depolymerization from well-defined polymers to monomers, J. Am. Chem. Soc. 145 (2023) 9898–9915.
[25] M.R. Martinez, K. Matyjaszewski, Degradable and recyclable polymers by reversible deactivation radical polymerization, CCS Chem. 4 (2022) 2176–2211.
[26] Y. Sano, T. Konishi, M. Sawamoto, M. Ouchi, Controlled radical depolymerization of chlorine-capped PMMA via reversible activation of the terminal group by ruthenium catalyst, Eur. Polym. J. 120 (2019) 109181.
[27] M.R. Martinez, S. Dadashi-Silab, F. Lorandi, Y.Q. Zhao, K. Matyjaszewski, Depolymerization of P(PDMS(11)MA) bottlebrushes via atom transfer radical polymerization with activator regeneration, Macromolecules 54 (2021) 5526–5538.
[28] J.F. Zhou, D. Sathe, J.P. Wang, Understanding the structure-polymerization thermodynamics relationships of fused-ring cyclooctenes for developing chemically recyclable polymers, J. Am. Chem. Soc. 144 (2022) 928–934.
[29] H.S. Wang, N.P. Truong, G.R. Jones, A. Anastasaki, Investigating the effect of end-group, molecular weight, and solvents on the catalyst-free depolymerization of RAFT Polymers: Possibility to reverse the polymerization of heat-sensitive polymers, ACS Macro Lett. 11 (2022) 1212–1216.
[30] J. Nicolas, Y. Guillaneuf, C. Lefay, D. Bertin, D. Gigmes, B. Charleux, Nitroxide-mediated polymerization, Prog. Polym. Sci. 38 (2013) 63–235.
[31] H.S. Wang, N.P. Truong, Z.P. Pei, M.L. Coote, A. Anastasaki, Reversing RAFT polymerization: Near-quantitative monomer generation via a catalyst-free depolymerization approach, J. Am. Chem. Soc. 144 (2022) 4678–4684.
[32] K. Matyjaszewski, Atom transfer radical polymerization (ATRP): Current status and future perspectives, Macromolecules 45 (2012) 4015–4039.
[33] S. Perrier, 50th Anniversary perspective: RAFT polymerization-a user guide, Macromolecules 50 (2017) 7433–7447.
[34] H.R. Lamontagne, B.H. Lessard, Nitroxide-mediated polymerization: A versatile tool for the engineering of next generation materials, ACS Appl. Polym. Mater. 2 (2020) 5327–5344.
[35] M.R. Martinez, F.D. Bossa, M. Olszewski, K. Matyjaszewski, Copper(II) chloride/tris(2-pyridylmethyl)amine-catalyzed depolymerization of poly(*n*-butyl methacrylate), Macromolecules 55 (2022) 78–87.
[36] F.D. Bossa, G. Yilmaz, K. Matyjaszewski, Fast bulk depolymerization of polymethacrylates by ATRP, ACS Macro Lett. 12 (2023) 1173–1178.
[37] M.R. Martinez, D. Schild, F.D. Bossa, K. Matyjaszewski, Depolymerization of polymethacrylates by iron ATRP, Macromolecules 55 (2022) 10590–10599.
[38] M.J. Flanders, W.M. Gramlich, Reversible-addition fragmentation chain transfer (RAFT) mediated depolymerization of brush polymers, Polym. Chem. 9 (2018) 2328–2335.
[39] F. Häfliger, N.P. Truong, H.S. Wang, A. Anastasaki, Fate of the RAFT end-group in the thermal depolymerization of polymethacrylates, ACS Macro Lett. 12 (2023) 1207–1212.
[40] R. Whitfield, G.R. Jones, N.P. Truong, L.E. Manring, A. Anastasaki, Solvent-free chemical recycling of polymethacrylates made by ATRP and RAFT polymerization: High-yielding depolymerization at low temperatures, Angew. Chem., Int. Ed. 62 (2023) e202309116.
[41] J.B. Young, R.W. Hughes, A.M. Tamura, L.S. Bailey, K.A. Stewart, B.S. Sumerlin, Bulk depolymerization of poly(methyl methacrylate) via chain-end initiation for catalyst-free reversion to monomer, Chem 9 (2023) 2669–2682.

[42] R.W. Hughes, M.E. Lott, I.S. Zastrow, J.B. Young, T. Maity, B.S. Sumerlin, Bulk depolymerization of methacrylate polymers via pendent group activation, J. Am. Chem. Soc. 146 (2024) 6217–6224.
[43] M.T. Chin, T.G. Yang, K.P. Quirion, C. Lian, P. Liu, J. He, T.N. Diao, Implementing a doping approach for poly(methyl methacrylate) recycling in a circular economy, J. Am. Chem. Soc. 146 (2024) 5786–5792.
[44] X.C. Pan, M.A. Tasdelen, J. Laun, T. Junkers, Y. Yagci, K. Matyjaszewski, Photomediated controlled radical polymerization, Prog. Polym. Sci. 62 (2016) 73–125.
[45] T. Chen, H.N. Wang, Y.Y. Chu, C. Boyer, J.Q. Li, J.T. Xu, Photo-induced depolymerisation: Recent advances and future challenges, ChemPhotoChem 3 (2019) 1059–1076.
[46] Z. Arslan, H.C. Kiliclar, Y. Yagci, Dimanganese decacarbonyl catalyzed visible light induced ambient temperature depolymerization of poly(methyl methacrylate), Des. Monomers Polym. 25 (2022) 271–276.
[47] J.B. Young, J.I. Bowman, C.B. Eades, A.J. Wong, B.S. Sumerlin, Photoassisted radical depolymerization, ACS Macro Lett. 11 (2022) 1390–1395.
[48] K. Parkatzidis, N.P. Truong, K. Matyjaszewski, A. Anastasaki, Photocatalytic ATRP depolymerization: Temporal control at low ppm of catalyst concentration, J. Am. Chem. Soc. 145 (2023) 21146–21151.
[49] V. Bellotti, K. Parkatzidis, H.S. Wang, N.D.A. Watuthanthrige, M. Orfano, A. Monguzzi, N.P. Truong, R. Simonutti, A. Anastasaki, Light-accelerated depolymerization catalyzed by Eosin Y, Polym. Chem. 14 (2023) 253–258.
[50] V. Bellotti, H.S. Wang, N.P. Truong, R. Simonutti, A. Anastasaki, Temporal regulation of PET-RAFT controlled radical depolymerization, Angew. Chem., Int. Ed. 62 (2023) e202313232.
[51] G. Szczepaniak, M. Lagodzinska, S. Dadashi-Silab, A. Gorczynski, K. Matyjaszewski, Fully oxygen-tolerant atom transfer radical polymerization triggered by sodium pyruvate, Chem. Sci. 11 (2020) 8809–8816.
[52] T. Scherzer, H. Langguth, Temperature dependence of the oxygen solubility in acrylates and its effect on the induction period in UV photopolymerization, Macromol. Chem. Phys. 206 (2005) 240–245.
[53] G. Ng, S.W. Prescott, A. Postma, G. Moad, C.J. Hawker, A. Anastasaki, C. Boyer, Enhancing photothermal depolymerization with metalloporphyrin catalyst, J. Polym. Sci. 1–9 (2024).
[54] S.A. Mountaki, R. Whitfield, E. Liarou, N.P. Truong, A. Anastasaki, Open-air chemical recycling: Fully oxygen-tolerant ATRP depolymerization, J. Am. Chem. Soc. 146 (2024) 18848–18854.
[55] F. Lorandi, M. Fantin, H. Jafari, A. Gorczynski, G. Szczepaniak, S. Dadashi-Silab, A. A. Isse, K. Matyjaszewski, Reactivity prediction of Cu-catalyzed halogen atom transfer reactions using data-driven techniques, J. Am. Chem. Soc. 145 (2023) 21587–21599.
[56] T. Pintauer, K. Matyjaszewski, Structural aspects of copper catalyzed atom transfer radical polymerization, Coord. Chem. Rev. 249 (2005) 1155–1184.
[57] T.G. Ribelli, M. Fantin, J.C. Daran, K.F. Augustine, R. Poli, K. Matyjaszewski, Synthesis and characterization of the most active copper ATRP catalyst based on tris (4-dimethylaminopyridyl)methyl amine, J. Am. Chem. Soc. 140 (2018) 1525–1534.
[58] T.G. Ribelli, F. Lorandi, M. Fantin, K. Matyjaszewski, Atom transfer radical polymerization: Billion times more active catalysts and new initiation systems, Macromol. Rapid Commun. 40 (2019) 1800616.
[59] W. Tang, Y. Kwak, W. Braunecker, N.V. Tsarevsky, M.L. Coote, K. Matyjaszewski, Understanding atom transfer radical polymerization: Effect of ligand and initiator structures on the equilibrium constants, J. Am. Chem. Soc. 130 (2008) 10702–10713.
[60] M. Cvek, A.M. Jazani, J. Sobieski, T. Jamatia, K. Matyjaszewski, Comparison of mechano- and photoATRP with ZnO nanocrystals, Macromolecules 56 (2023) 5101–5110.
[61] S.A. Mountaki, R. Whitfield, K. Parkatzidis, M.N. Antonopoulou, N.P. Truong, A. Anastasaki, Chemical recycling of bromine-terminated polymers synthesized by ATRP, RSC Appl. Polym. 2 (2024) 275–283.
[62] J.H. Xia, K. Matyjaszewski, Controlled/"living'' radical polymerization. Atom transfer radical polymerization catalyzed by copper(I) and picolylamine complexes, Macromolecules 32 (1999) 2434–2437.
[63] A.K. Nanda, K. Matyjaszewski, Effect of PMDETA / Cu(I) ratio, monomer, solvent, counterion, ligand, and alkyl bromide on the activation rate constants in atom transfer radical polymerization, Macromolecules 36 (2003) 1487–1493.
[64] J.S. Wang, K. Matyjaszewski, Controlled living radical polymerization - Atom transfer radical polymerization in the presence of transition-metal complexes, J. Am. Chem. Soc. 117 (1995) 5614–5615.
[65] F.D. Bossa, K. Matyjaszewski, How to reverse radical polymerization back to monomers in a controlled way, Chem 10 (2024) 26–29.
[66] X.M. Xu, X. Xu, Y.N. Zeng, F.A. Zhang, Oxygen-tolerant photo-induced metal-free atom transfer radical polymerization, J. Photochem. Photobiol., A 411 (2021) 113191.
[67] M. Sys, A. Mukherjee, G. Jashari, V. Adam, A.M. Ashrafi, M. Novák, L. Richtera, Bis (2,2′-bipyridil)copper(II) chloride complex: Tyrosinase biomimetic catalyst or redox mediator? Materials 14 (2021) 113.
[68] B. Knuehl, T. Pintauer, A. Kajiwara, H. Fischer, K. Matyjaszewski, Characterization of Cu(II) bipyridine complexes in halogen atom transfer reactions by electron spin resonance, Macromolecules 36 (2003) 8291–8296.
[69] J. Yeow, R. Chapman, A.J. Gormley, C. Boyer, Up in the air: Oxygen tolerance in controlled/living radical polymerisation, Chem. Soc. Rev. 47 (2018) 4357–4387.
[70] R.A. Johnson, E.G. Nidy, M.V. Merritt, Superoxide chemistry - Reactions of superoxide with alkyl-halides and alkyl sulfonate esters, J. Am. Chem. Soc. 100 (1978) 7960–7966.
[71] K. Parkatzidis, N.P. Truong, R. Whitfield, C.E. Campi, B. Grimm-Lebsanft, S. Buchenau, M.A. Rübhausen, S. Harrisson, D. Konkolewicz, S. Schindler, A. Anastasaki, Oxygen-enhanced atom transfer radical polymerization through the formation of a copper superoxido complex, J. Am. Chem. Soc. 145 (2023) 1906–1915.
[72] A.M. Jazani, D.J. Schild, J. Sobieski, X.L. Hu, K. Matyjaszewski, Visible light-ATRP driven by tris(2-pyridylmethyl)amine (TPMA) impurities in the open air, Macromol. Rapid Commun. 44 (2022) 2200855.
[73] Y. Kwak, K. Matyjaszewski, ARGET ATRP of methyl methacrylate in the presence of nitrogen-based ligands as reducing agents, Polym. Int. 58 (2009) 242–247.
[74] E. Frick, A. Anastasaki, D.M. Haddleton, C. Barner-Kowollik, Enlightening the mechanism of copper mediated photoRDRP via high-resolution mass spectrometry, J. Am. Chem. Soc. 137 (2015) 6889–6896.
[75] T.G. Ribelli, D. Konkolewicz, S. Bernhard, K. Matyjaszewski, How are radicals (re) generated in photochemical ATRP? J. Am. Chem. Soc. 136 (2014) 13303–13312.
[76] A.M. Jazani, C. Rawls, K. Matyjaszewski, Photo-RDRP for everyone: Smartphone light-induced oxygen-tolerant reversible deactivation radical polymerization, Eur. Polym. J. 202 (2024) 112631.
[77] J.T. Xu, S. Shanmugam, H.T. Duong, C. Boyer, Organo-photocatalysts for photoinduced electron transfer-reversible addition-fragmentation chain transfer (PET-RAFT) polymerization, Polym. Chem. 6 (2015) 5615–5624.
[78] P. Chaibuth, N. Chuaytanee, J. Hojitsiriyanont, K. Chainok, S. Wacharasindhu, O. Reiser, M. Sukwattanasinitt, Copper(II) complexes of quinoline-based ligands for efficient photoredox catalysis of atom transfer radical addition (ATRA) reaction, New J. Chem. 46 (2022) 12158–12168.
[79] J. Hu, J. Wang, T.H. Nguyen, N. Zheng, The chemistry of amine radical cations produced by visible light photoredox catalysis, Beilstein J. Org. Chem. 9 (2013) 1977–2001.
[80] D. Bondarev, K. Borska, M. Soral, D. Moravcikova, J. Mosnacek, Simple tertiary amines as promotors in oxygen tolerant photochemically induced ATRP of acrylates, Polymer 161 (2019) 122–127.
[81] H.F. Piedra, C. Valdes, M. Plaza, Shining light on halogen-bonding complexes: A catalyst-free activation mode of carbon-halogen bonds for the generation of carbon-centered radicals, Chem. Sci. 14 (2023) 5545–5568.
[82] G.X. Zhang, Z.N. Zhang, R. Zeng, Photoinduced $FeCl_3$-catalyzed alkyl aromatics oxidation toward degradation of polystyrene at room temperature, Chin. J. Chem. 39 (2021) 3225–3230.
[83] S. Oh, E.E. Stache, Chemical upcycling of commercial polystyrene via catalyst-controlled photooxidation, J. Am. Chem. Soc. 144 (2022) 5745–5749.